N75-12758

PAPER 4.6

THE AIROSCOPE POINTING AND STABILIZATION SYSTEM

James P. Murphy
Kenneth R. Lorell
Ames Research Center

ABSTRACT

The AIROscope pointing and stabilization system is described. The system is configured with three gimbal axes and rate integrating gyro stabilization to provide a stable platform for infrared astronomy. Error signals for on and off-axis pointing are derived from a video sensor which also drives a ground station display. Other features of the system include direct drive torque motors and electronic suspension damping. Results of analysis and simulations used to design the control loops, and a pointing error analysis are presented.

INTRODUCTION

The AIROscope pointing and stabilization system has been designed to allow a variety of infrared investigations. The system has the capability to scan selected sky regions and to point for extended periods of time at visible infrared (IR) objects (on-axis pointing) or at IR objects that have no visible counterpart (off-axis pointing).

Key features of the system hardware include rate integrating gyro (RIG) stabilization of three gimbal axes; azimuth, elevation and cross elevation. Direct drive dc torgue motors control the elevation and cross elevation axes, and a dc torque motor and tachometer are used for suspension damping and control of the azimuth axis. A unique video sensor and associated electronics provide error signals for on and off-axis pointing. A control panel in the ground station commands the pointing and stabilization system and includes a CRT display for presentation of the video sensor output and a joystick for commanding slew rates to the elevation and cross elevation RIG's.

The system has two primary pointing modes that can be selected at the ground station, manual and TV auto. In the manual mode, the CRT display and joystick are used to control pointing of the telescope; in the TV auto mode, error signals from the video sensor control the pointing of the telescope. While pointing accuracy in the manual mode depends on the ability of the operator, the system has the capability to move minutes of arc in a controlled fashion. In the TV auto mode for on-axis pointing, pointing accuracy is expected to be less than 0.51 arc minutes, and for off-axis pointing, pointing accuracy is expected to be less than 1.29 arc minutes for time periods up to 1 hour.

SYSTEM CONFIGURATION

The system has been configured to satisfy the requirements of infrared astronomy. Since off-axis pointing is essential, the effect of gondola

disturbances on the rotation of the telescope axis is important. While a simpler two gimbal platform (Greeb et. al., 1974) could have been used, a three gimbal platform, with RIG stabilization for each gimbal axis, was selected to provide better isolation of the telescope from suspension and gondola disturbances such as pendulation. Figure 1 shows the AIROscope gimbal arrangement and the location of the primary pointing and stabilization hardware on the azimuth, elevation and cross elevation gimbals.

The mounting location of the RIG's on the gimbals has been chosen as a compromise between complexity and performance. All three RIG's could have been mounted on the telescope to provide complete stabilization similar to an inertial platform, however, this would require a complex coordinate transformation to derive the error signals to drive the torque motors. In addition, a gingularity would exist when the cross elevation and azimuth axes are parallel at low elevation angles. Consequently, the elevation and cross elevation RIG's are mounted on the telescope, and the azimuth RIG is mounted on the azimuth gimbal. The RIG's chosen for the system are surplus units which can be trimmed electronically to have drift rates below 1 degree/hour and which have a noise level of 2 to 3 degrees/hour rms.

Direct drive dc torque motors supply control torques for the three gimbal axes. Even though direct drive torque motors require more power than geared dc torque motors, the direct drive motors allow more isolation from gondola disturbances and better pointing stability. A toothless gear train has been used (Frecker, 1968) in a previous balloon system to eliminate the backlash associated with standard gears, however, the gimbals are still directly coupled to the gondola because of the necessity to accelerate the gear train. With the direct drive motors, the only coupling to the gondola is through bearing stiction and motor back-emf. Pairs of dc direct drive motors are utilized for both the elevation and cross elevation axes to reduce the effect of mechanical resonances (Frecker, 1968). A single dc torque motor is used for azimuth and torques against the suspension. Since the suspension acts as a lightly damped spring inertia system, a tachometer is used to measure the relative rate between the suspension and gondola, and control logic is implemented which increases the damping of the suspension.

The primary attitude sensor for the system is a unique video sensor whose error signals control the elevation and cross elevation RIG's for the TV auto pointing mode and provide information for the CRT display in the ground station. A complete description of the video sensor system is given by Deboo et. al. (1974). As a backup to the video sensor, a star tracker is available which can be used for on-axis pointing. Alignment of the video sensor and star tracker to the telescope is done prior to flight and experience has shown that the alignment can be accomplished and held during flight to within 0.5 arc minutes (Scott, 1974). While the primary reference for the azimuth gimbal is a RIG, it is not a satisfactory long term attitude reference. Consequently, a compass is mounted on the azimuth gimbal and a readout of azimuth attitude with respect to magnetic north is provided in the ground station.

A control panel in the ground station is used to command the pointing and stabilization system and includes a visual presentation of the video

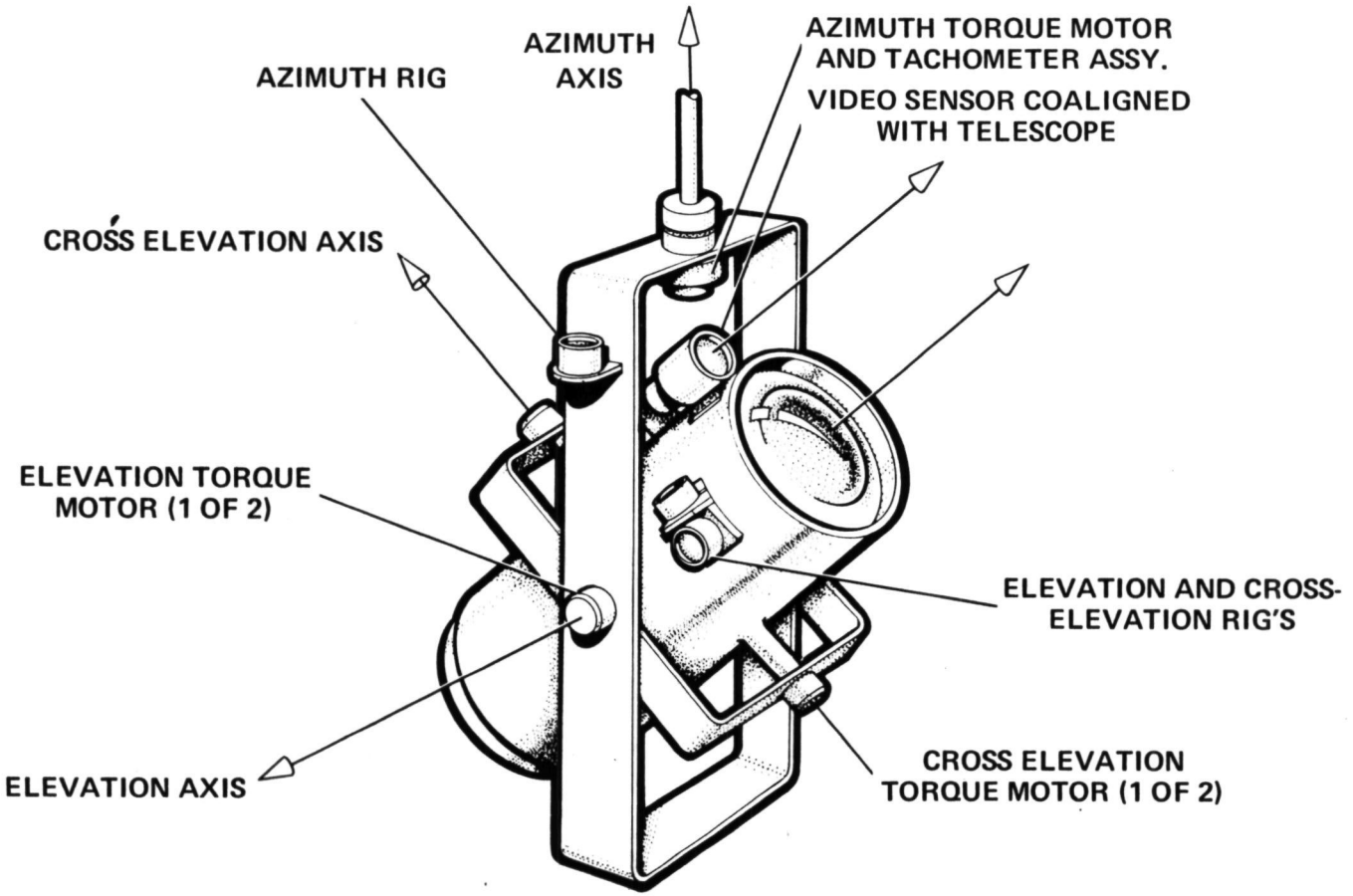

Figure 1. AIROscope Gimbal Configuration

sensor output. A joystick commands slew rates to the elevation and cross elevation RIG's for manual pointing, and is used with the TV auto mode to control the gate positions in the video sensor's gate electronics. A rotary switch selects the pointing modes and thumbwheel switches control the selection of bias currents for compensating the RIG drifts. A thumbwheel switch also commands the desired azimuth attitude.

AZIMUTH CONTROL LOOP

Coarse acquisition of IR targets is accomplished by slewing the azimuth gimbal with reference to magnetic north. Once the gimbal has stabilized at the commanded angle, a stabilization mode, which isolates the telescope from axial motion of the balloon and suspension, commences. Small adjustments (approx. 1.5°-2°) may be made during stabilization but the control must be returned to the slew mode for large angle changes. The primary attitude sensor is a RIG, located on the gimbal, whose sensitive axis is coincident with the azimuth axis. A reference to the earth's magnetic vector is provided by a magnetic compass.

The design of the azimuth gimbal pointing and stabilization loop was influenced by a number of considerations arising from both the disturbance-torque environment in which the system operates, and the system configuration. Primary among these are the need to damp the motion of the suspension and to compensate for the combined effects of balloon rotation and bearing friction, both viscous and static. Additional design constraints derive from the need to decouple the motion of the suspension from the gondola as much as possible during stabilization and to provide an angular reference during the slew mode.

There are two major physical phenomena with which the aximuth controller must contend: first, disturbances transferred from the suspension to the gondola through the azimuth gimbal bearing; and second, the large amplitude oscillations of the suspension excited by torque motor impulses. At float altitude, the balloon attains a relatively steady state rotation, the sense of the spin being unpredictable, of .25°/sec to 1.0°/sec (Morris, 1969), which results in a steady rotation of the suspension as well. This motion of the suspension is translated into a relatively constant body-fixed torque on the gondola azimuth axis through the action of viscous bearing friction, damping terms in the control law, torque motor back-emf and the non-negligible amount of stiction in the bearing (Nidey, 1969, Nidey, 1966). The use of a conventional rate-plus-position control law to stabilize the azimuth gimbal, while providing adequate damping and slewing control, results in steady-state errors in the commanded azimuth angle proportional to body-fixed moments applied to the gondola. Therefore, in order to maintain little or no offset, some additional compensation is necessary.

Control torque along the axis of the azimuth gimbal is provided by a torque motor acting directly against the cables used to suspend the gondola from the balloon. The suspension behaves like a very lightly damped torsional spring-mass system when excited by the azimuth torque motor. In order to keep from "wrapping up" the suspension (i.e., causing the cables to cross, thus reducing the effective spring constant to zero) and eliminate

the large oscillations that result from torque pulses, a control law that includes terms to damp motion of the suspension should be employed.

Precise pointing of the telescope requires that the effects of disturbances to the gondola be minimized. Thus, during the stabilization mode, it is desirable to decouple the gondola from the suspension as much as possible. This is in contrast to the requirement that the suspension be damped to avoid wind-up and large-amplitude oscillations. Therefore, the controller should be mechanized in a way that provides two levels of suspension damping in order to satisfy both slewing and stabilization requirements.

For reasons discussed earlier, a RIG was selected as the primary attitude sensor for use during stabilization. It would be desirable to use the RIG as the attitude sensor during the slew mode as well, thereby conserving weight, power, and complexity. However, most RIG's have only limited (usually less than 10°) motion about the sensing axis precluding their use for slewing through large angles. Thus, an additional consideration is the modification of the characteristics of a RIG during acquisition of targets through large angles.

Figure 2 shows the AIROscope gondola suspended from the balloon by two cables 55.8m in length. The axial reaction moment of the suspension-gondola system is a function of the cable length L, the gondola mass m, the angle through which the suspension is twisted relative to the balloon θ_r, and the distance separating the two cables d.

Thus

$$K_\theta = \frac{2mgL}{\theta_r^2}\left[1 - \left(1 - \frac{d^2}{L^2}\,\mathrm{SIN}^2\,\frac{\theta_r}{2}\right)\right]$$

where K_θ

represents the classical spring "constant." A curve of K_θ vs. θ_r assumes the shape of a parabola with the maximum occurring around $\theta_r = 0$. For the purposes of this analysis, K_θ will be considered a constant, its value calculated at $\theta_r = 45°$. A design goal is to constrain θ_r from exceeding ± 30.°

A simple model of the system to be controlled is illustrated in figure 3.

For a linear system:

$$J_1\ddot{\theta}_1 = -K_\theta\theta_1 - K_B(\dot{\theta}_1 - \dot{\theta}_2) - M_C + M_{D1}$$

$$J_2\ddot{\theta}_2 = -K_B(\dot{\theta}_2 - \dot{\theta}_1) + M_C + M_{D2}$$

A conventional method of providing damping for the suspension would be to use $\dot{\theta}_1$ as part of the control law. Although it is not practical to measure $\dot{\theta}_1$ directly, by putting a tachometer on the torque motor shaft, $\dot{\theta}_2 - \dot{\theta}_1$ can be measured. θ_2 and $\dot{\theta}_2$ are available from the sensor on the azimuth gimbal, so a rate-plus-position linear control law would give:

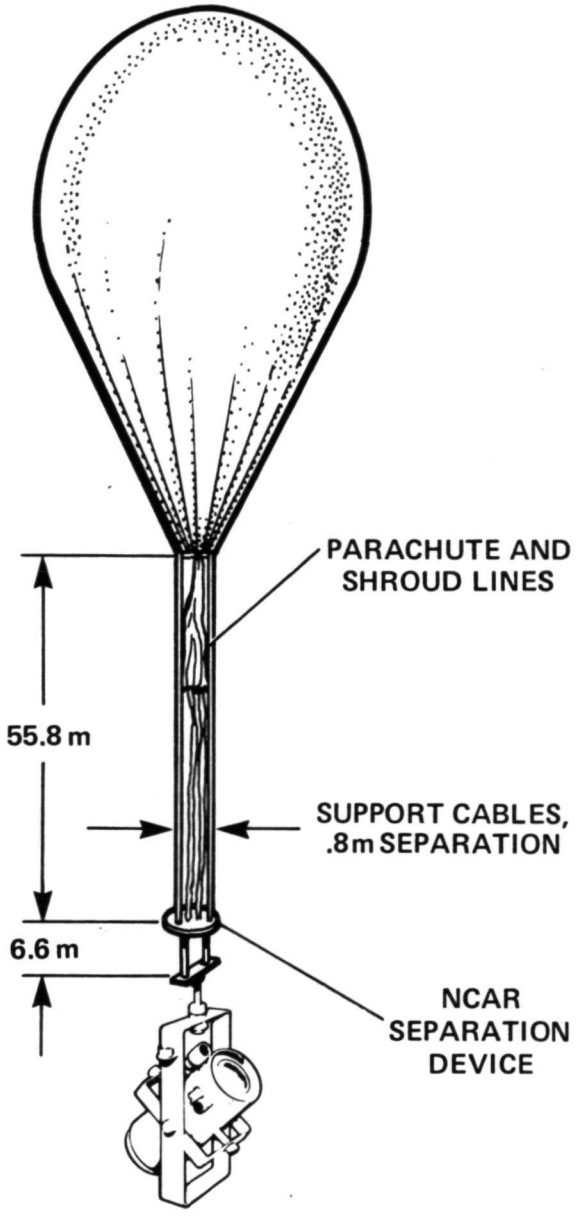

Figure 2. AIROscope Suspension Configuration

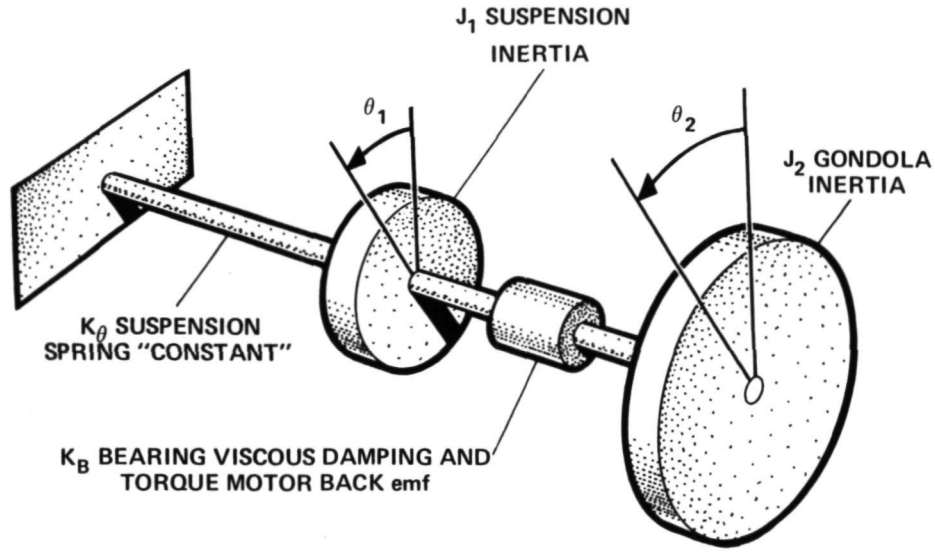

Figure 3. Simple Dynamic Model of AIROscope Suspension Coupled to Gondola

$$J_1\ddot{\theta}_1+(K_B+K_B')\dot{\theta}_1+K_\theta\theta_1 = (K_B+K_B'+K_V)\dot{\theta}_2 + K_P\theta_2+M_{D1}$$

$$J_2\ddot{\theta}_2+(K_B+K_B'+K_V)\dot{\theta}_2+K_P\theta_2 = (K_B+K_B')\theta_1+M_{D2}$$

We can control suspension damping through K_B' and adjust the aximuth damping coefficient through $(K_B' + K_V)$. The response of the two systems cannot be controlled arbitrarily because of the coupling, so gain selection requires a compromise between fast response of the gondola and adequate damping of the suspension.

The steady-state rotation of the balloon may be modelled as a ramp torque acting on the suspension. Bearing stiction is a disturbance of fixed magnitude whose sign depends on the sign of $(\dot{\theta}_1-\dot{\theta}_2)$. So,

$$M_{D1} = K_\theta(K_R t) - \text{SGN}\ (\dot{\theta}_1-\dot{\theta}_2)M_S,\ M_D = \text{SGN}\ (\dot{\theta}_1-\dot{\theta}_2)M_S$$

Substituting M_{D1} and M_{D2} into the equations above and Laplace transforming them, we can obtain steady-state solutions for θ_1 and θ_2.

$$\theta_1\ (t\to\infty)\to\infty$$

$$\dot{\theta}_1\ (t\to\infty) = K_R$$

$$\theta_2\ (t\to\infty) = \frac{(K_B+K_B')K_R+M_S}{K_P}$$

As expected, the quality of the bearing between the suspension and the azimuth gimbal is a major factor influencing the pointing performance of the system. If an estimate of the offset torque $(K_B+K_B')K_R+M_S$ could be made, it would be possible to eliminate the offset.

In order to provide azimuth rate and position information during the slew mode, some form of reference other than the azimuth gimbal RIG must be used for reasons stated earlier. A rate gyro whose output is integrated to provide position will satisfy this requirement. However, rather than add a rate gyro to the system, the RIG may be made to behave like a rate gyro by electronically closing the loop between its output-axis position pick-off and torquer. By selecting K_G in

$$J_3\ddot{\phi} + K_Z\dot{\phi} + K_G\phi = \dot{\theta}_2 H$$

so that the gyro has the appropriate step response as well as steady-state error to ramp inputs as given by

$$\varepsilon\ (t\to\infty) = \frac{K_Z}{K_G}\cdot K_a,$$

(where K_a is an arbitrary constant acceleration), a rate gyro of relatively low but sufficient bandwidth for this system is produced.

Angular reference is provided by integrating the output of the rate gyro. A digital integrator, consisting of a voltage-to-frequency converter, an up-down counter, and a digital to analogue converter is employed. This mechanization has the advantages of low drift, wide dynamic range, and the capability of accepting command angle inputs directly from the command system.

When a two mode system is used, mode I for slewing to the commanded azimuth angle and mode II for stabilization, the problems of dual suspension damping coefficients and RIG vs. rate gyro operation are alleviated. While slewing, a large damping coefficient K'_{B1} is provided to keep the suspension motion relatively subdued. The RIG gimbal is always nulled by closure of the pickoff-torquer loop converting it to a rate gyro. An integrator connected to its output supplies the attitude reference. After $\dot{\theta}_2$, the angular velocity of the azimuth axis measured by the rate gyro, has remained below some low threshold value for an appropriate length of time, the controller can be switched to mode II for stabilization.

In mode II operation, the damping gain for the suspension can be decreased by an order of magnitude (K'_{B2}) to give adequate damping for the low levels of torque motor activity while improving the isolation of the suspension from the gondola. The gyro is returned to the RIG configuration by disconnecting the gain K_G. Control signals are taken from the RIG output and compensated by a lead-lag network.

A conventional controller would also bypass the integrator, since its output is no longer necessary with the RIG in the loop. However, such a system with the integrator disconnected will exhibit a steady state error in mode II of up to 6° for a balloon rotation rate of .6°/sec and typical values of K_B, K'_{B2}, K_P and M_S. This is clearly unacceptable in view of the ± 10° angular freedom of the cross elevation gimbal.

An earlier equation shows that $K_P\theta_2(t\to\infty) = (K_B+K'_{B1})K_R+M_S$, or that the steady state value of the position error signal is an estimate of the disturbing moment. Further, the value of θ_2 stored in the integrator subtracted from the commanded azimuth angle represents the pointing error of the control system attained during mode I. Thus, two changes to a standard control loop can correct this pointing offset. First, after the integrator input is disconnected, the integrator output is retained as part of the control signal. Second, the output of the RIG, which in mode II supplies position information, can be biased with the error value of $\theta_2(t\to\infty)$ stored in the integrator in order to point the gondola back towards its original commanded azimuth angle. If $\theta_2^I(t\to\infty)$, $\theta_2^{II}(t\to\infty)$ represent the steady state values of θ_2 at the end of modes I and II respectively, then

$$\theta_2^I(t\to\infty)K_{P1} = (K_B+K'_{B1})K_R + M_S$$

and

$$\theta_2^{II}(t\to\infty)K_{P2} = (K_B + K'_{B2})K_R + M_S - \theta_2^{I}(t\to\infty)K_{P1} - K_{P2}\theta_2^{I}(t\to\infty)$$

so that

$$\theta_2^{II}(t\to\infty)K_{P2} = (K'_{B2} - K'_{B1})K_R - K_{P2}\theta_2^{I}(t\to\infty)$$

By the addition of a sample-and-hold device, the only component not required in a conventional controller without the pseudo-integral control feature, the steady state value of the suspension rotation rate K_R can be obtained to compensate for the change in the damping value from K'_{B1} to K'_{B2}. This addition produces

$$\theta_2^{II}(t\to\infty)K_{P2} = (K'_{B2}-K'_{B1})K_R - (K'_{B2}-K'_{B1})K_{R(measured)} - K_{P2}\theta_2^{I}(t\to\infty)$$

or $\theta_2^{II}(t\to\infty)$ is biased to an equal and opposite value of the mode I pointing error.

Figures 4, 5, 6 illustrate the details of the azimuth controller. Figure 4 is a block diagram of the system showing the switches required to implement two-mode operation. Figure 5 is a simulated response of θ_2 to a 10° step slewing command. Note the 20-second timeout for $\dot{\theta}_2$ below the .05°/sec threshold and the correction of the attitude error in mode II. In Figure 6, θ_1 is shown for the same case of a 10° step slew command. The behavior is well damped at all times and does not exhibit the large angular excursions usually associated with slewing torques. Transition to mode II is characterized by a transient disturbance which is quickly removed with the K'_{B2} damping term. The steady state motion of the suspension is indicated by a line whose slope is K_R.

ELEVATION AND CROSS ELEVATION CONTROL LOOPS

The elevation and cross elevation control axes are identical except that cross elevation has a smaller inertia. In the manual pointing mode, slew commands enter the control axes as RIG torquing currents commanded with the joystick in the ground station. For the auto pointing mode, torque commands are provided to the RIG's from the video sensor. The output of the RIG is demodulated, filtered and then enters the RIG stabilization loop compensation. The control signal is then converted to a high power signal in the power amplifier and used to drive the torque motors. Figure 7 shows a block diagram of the elevation control axis. Simulations have been performed to design and evaluate the performance of the elevation and cross elevation control axes.

Figure 8 shows a bode plot of the RIG stabilization loop. The compensation is designed so that the open loop bode plot has a crossover frequency midway between the estimated mechanical natural frequency of the gimbal and telescope, and the estimated frequency of the pendulation disturbances. The compensation is complex and includes an electronic integration. Figure 9 shows a response of the RIG stabilization loop to

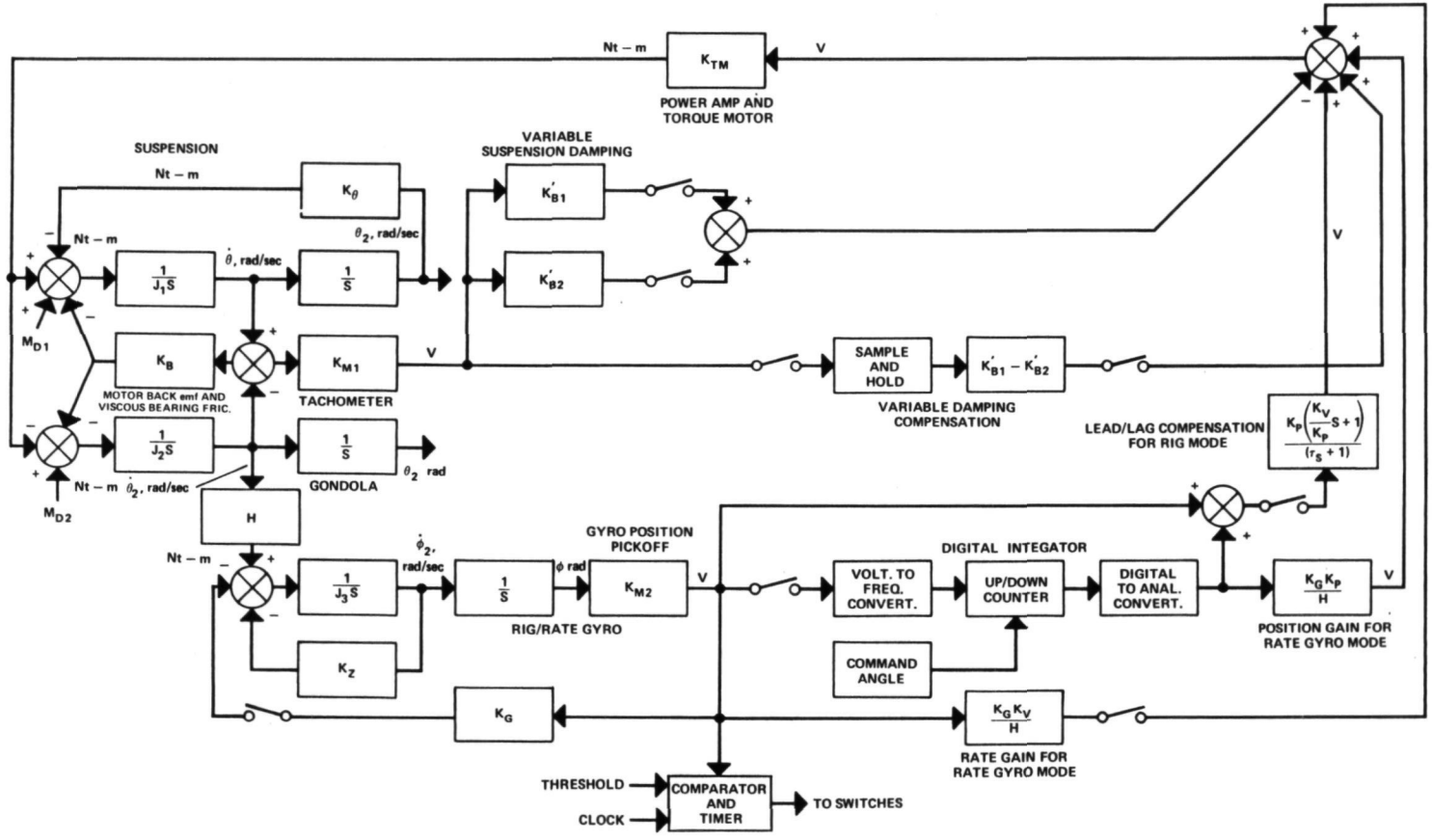

Figure 4. Azimuth Control System Block Diagram

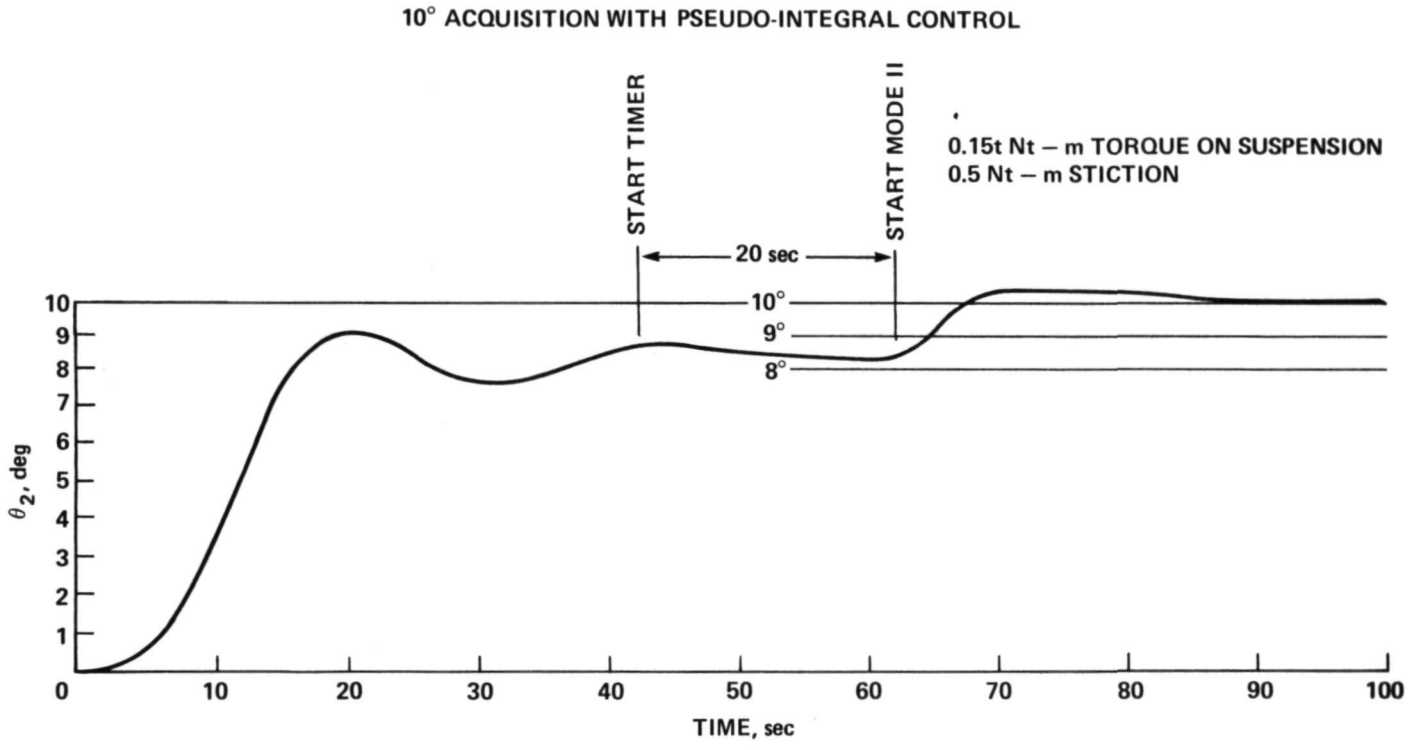

Figure 5. θ_2 versus Time

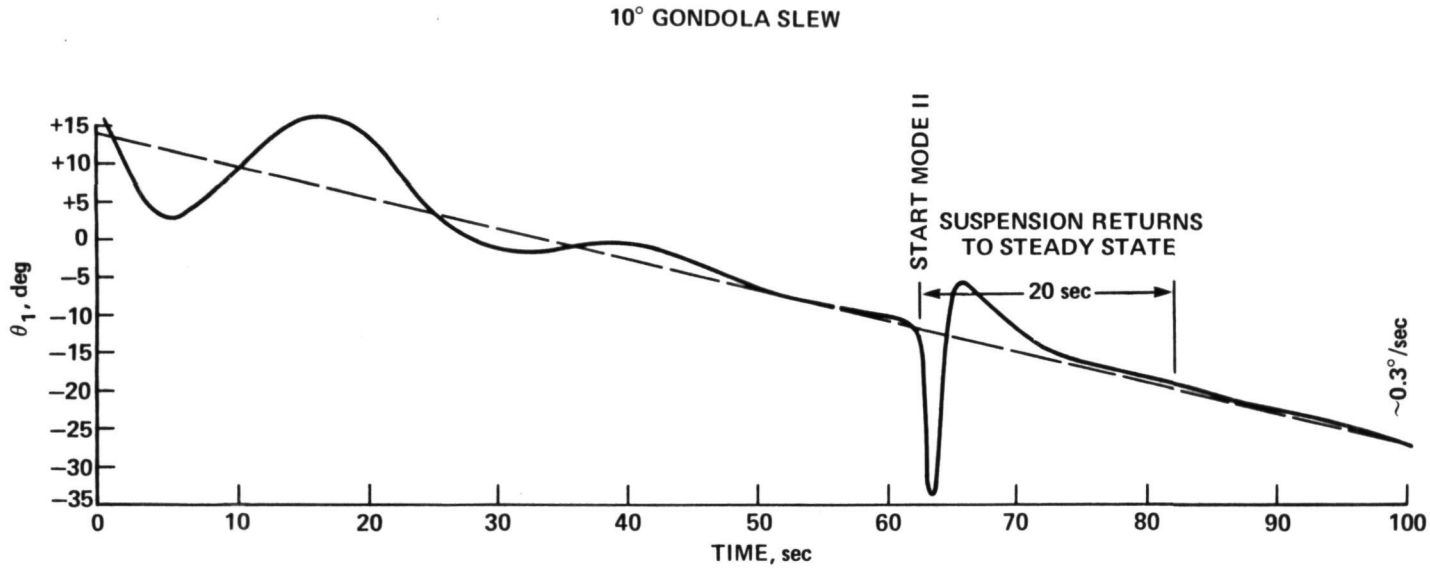

Figure 6. θ_1 versus Time

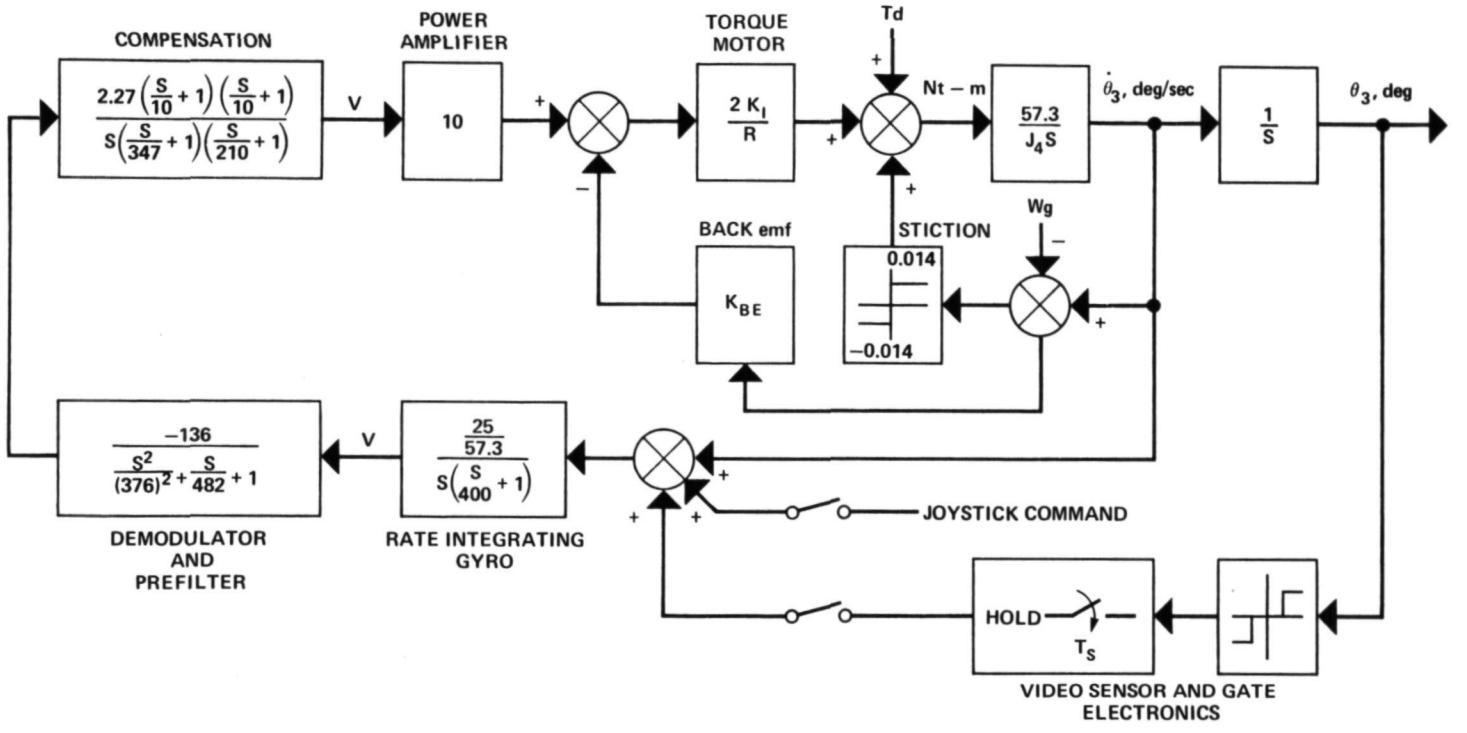

Figure 7. Elevation and Cross Elevation Control System Block Diagram

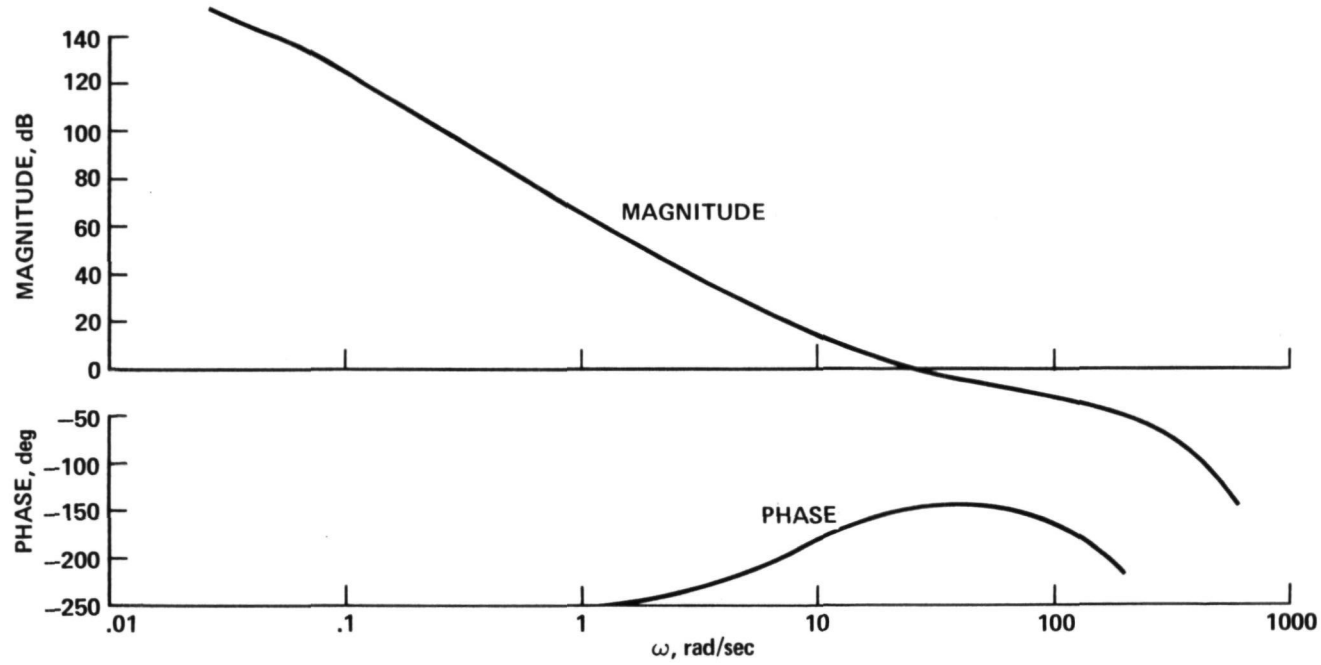

Figure 8. Bode Plot of RIG Stabilization Loop

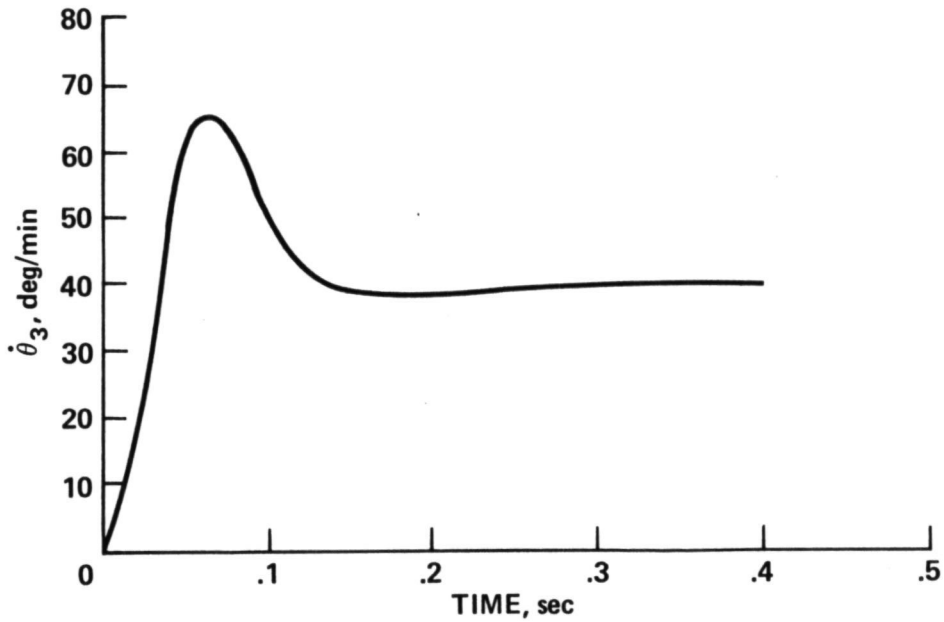

Figure 9. Response to Joystick Command

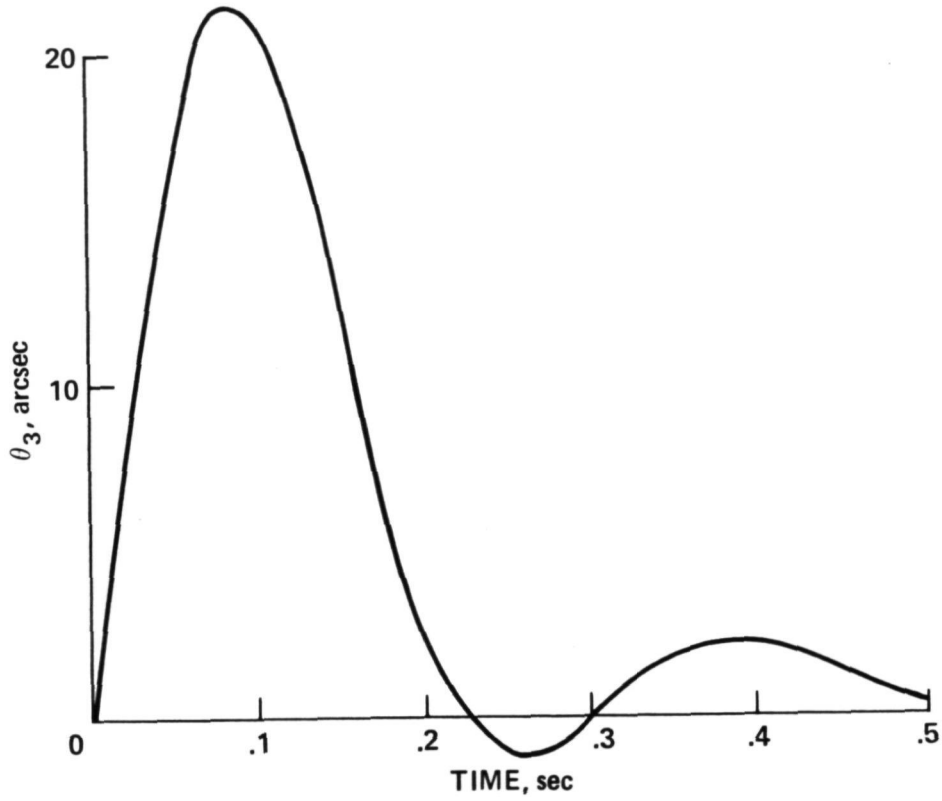

Figure 10. Response to Step Disturbance Torque

a step joystick command of 40 degrees/minute, while Figure 10 shows a response to a step disturbance torque of 1.4 nt.-m. A short time after application of the disturbance torque, the system returns to its original attitude. This effect is a result of the electronic integration in the compensation. Without the electronic integration, a steady state attitude change would result from the disturbance torque.

Since isolation of the telescope from the disturbances of the gondola is important for good stabilization performance, the RIG stabilization loop was tested for its ability to reject these disturbances. As shown in Figure 7, the primary coupling of the elevation or cross elevation axes to the gondola is through the motor back-emf and through bearing stiction. Figure 11 shows the response of the RIG stabilization loop to an oscillatory disturbance rate representing a pendulous motion of the gondola. At the lower pendulation frequency, the primary disturbance effect is caused by the bearing stiction; while, at the higher frequency the torque motor back-emf is the primary disturbance effect. Since the estimated compound pendulation frequency should be less than .5 Hz., the pointing stability caused by the stiction and back emf should be less than 5 arc seconds peak to peak.

A simulation was also performed of the RIG stabilization loop with RIG commands coming from the video sensor. This simulation was used to evaluate the performance of the TV auto mode with disturbance torques and RIG drift, and to choose a value for the torque commands from the video sensor. As shown in Figure 7, the video sensor has been simulated as a deadband with a sample-and-hold. The deadband corresponds to the adjustable gate size while the sample-and-hold results from the camera scan rate. With the simulation, RIG commands up to 120 degrees/hour were used with a deadband as small as ± 0.5 arc minute and no problems were experienced. With a RIG drift, limit cycle operation results and the frequency of cycling depends on the size of the drift. The result of a step disturbance torque is to cause a momentary RIG command; after a short period of time the system returns to normal. Figure 12 shows the acquisition from an initial condition of 6 arc minutes with a deadband of ± 0.5 arc minute and a RIG command of 120 degrees/hour. At t=4 seconds a step of disturbance torque is applied and results in a momentary RIG command; at t=10 seconds a RIG drift of 15 degrees/hour is applied and results in a periodic application of the RIG command.

POINTING ERROR SOURCES

A number of factors related to the mechanization and operating environment of the pointing and stabilization system contribute to the system pointing accuracy.

When the system is in the manual mode, i.e., joystick commands to the elevation and cross elevation RIG's, pointing accuracy is not as important as the ability to change the telescope attitude by very small amounts. The basic slow RIG command from the joystick is 1 degree/minute. Since the minimum command pulse time through the command system is approximately 0.1 second, a momentary joystick command would result in a telescope movement of 0.1 arc minutes. In addition, the low value of system jitter and stability provided by the direct drive motors and RIG stabilization, and the small trimmed RIG drift rates (below 1.0 degrees/hour) are also important for good performance in the manual pointing mode.

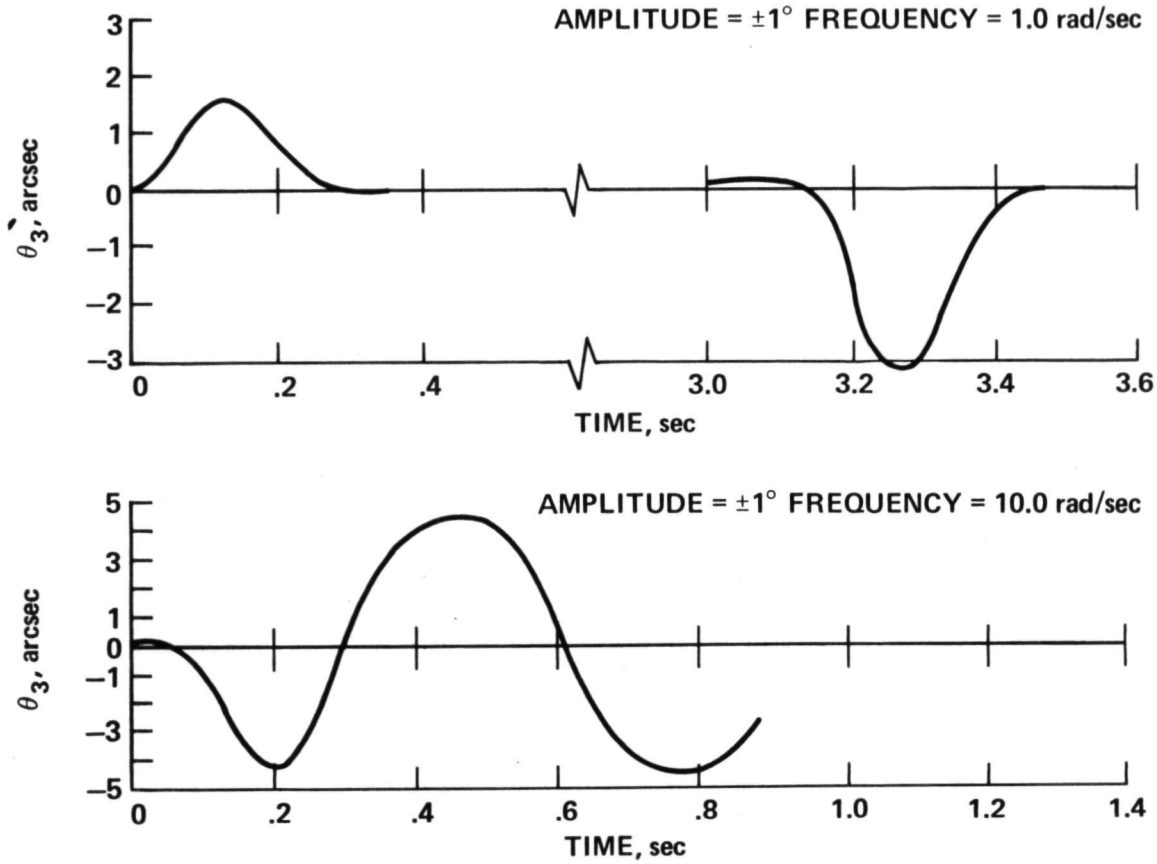

Figure 11. Response to Pendulation Disturbance

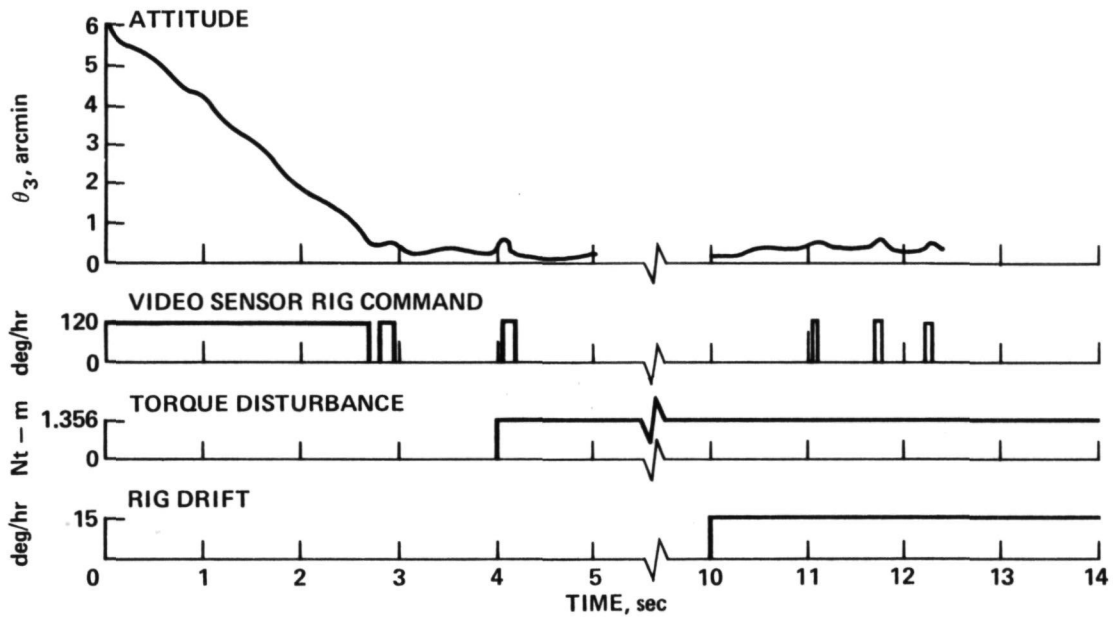

Figure 12. Attitude Response with Disturbance Torque and RIG Drift

In the TV auto pointing mode, pointing accuracy depends on whether the object can be tracked on or off-axis. If an IR object has a visible counterpart so that it can be tracked on-axis, the primary pointing errors are the misalignment of the video sensor to the telescope and the size of the deadband set in the video sensor's gate electronics. Since misalignments can typically be kept less than 0.5 arc minutes and the deadband can be set as small as ± 0.25 arc minutes, the worst case pointing error is less than 0.85 arc minutes. Figure 13 shows the error sources for on-axis pointing in the TV auto mode. Figure 14 shows the addition of the misalignment and deadband errors in a probablistic sense and shows that the error will be less than 0.51 arc minutes 68 percent of the time.

For off-axis pointing at IR objects in the TV auto mode, the video sensor gates must be positioned about a guide star in the field of view of the video sensor. While the same error sources for on-axis pointing affect the off-axis pointing accuracy, there are additional errors caused by nonlinearities in the video sensor and diurnal motion of the guide star.

To initiate off-axis auto pointing, the joystick and video display are used to position the desired object in the telescope field of view. When a sufficient indication of the object is obtained from the output of the experiment, the RIG's are used to hold the pointing position momentarily while the operator positions the video sensor electronic gates about a suitable guide star with the joystick. Since the video display in the ground station will have its own nonlinearities and null offsets, a set of lights in the ground station indicate whether the guide star is centered in the video sensor gate deadband on board the gondola. When the lights indicate that the gates are centered about the guide star, the TV auto mode is initiated. Consequently, pointing errors at the start of off-axis pointing are similar to the errors for on-axis pointing.

The guide star will appear to rotate about the desired object due to diurnal motion. The ability to move the null position of the gates to account for the diurnal motion will introduce additional errors over the time period required to obtain data from the science instrument. In addition, the diurnal motion will introduce errors due to linearity of the video sensor.

There are three methods that can be used to update the position of the gates due to diurnal motion. The first method would use sidereal time, right ascension and declination of the object and guide star, and latitude information to generate tables that could be used to obtain the position of the guide star relative to the target object as a function of time. Due to variations in time and latitude and the three gimbal angles associated with the gondola, it is apparent that the table look up method is somewhat cumbersome and inaccurate. A second, more precise method would use current information about the gondola gimbal angles, latitude, and time, combined with the right ascension and declination of the guide star and object to calculate in real time the video sensor gate positions. This method, while very accurate, would require a computer in the ground station with an electrical interface to the command and data systems.

A third method was developed which provides a compromise between hardware complexity and accuracy. This method uses the current gimbal angles, azimuth, elevation and cross elevation and latitude to find the component of earth rate about the telescope axis. This rate, the instantaneous rate at

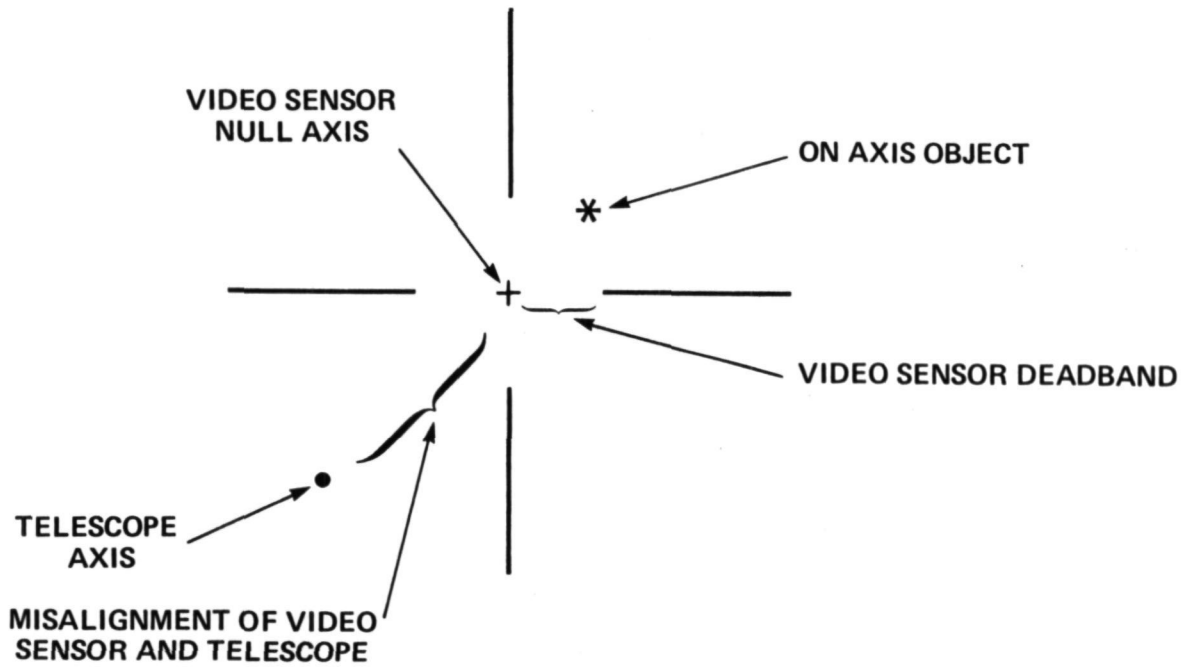

Figure 13. On-Axis Pointing Error Sources

ERROR SOURCE	arcmin	CONFIDENCE	1σ
MISALIGNMENT	0.50	1σ	0.50
GATE DEADBAND	0.35	3σ	0.12

1 σ RSS TOTAL = 0.51 arcmin

Figure 14. On-Axis Pointing Error

which the guide star is rotating about the pointing axis, is small (less than 15°/hour) and changes slowly. Knowledge of the present gate location combined with the value of the guide star rotation rate, allows the gate positions to be updated incrementally and these calculations can be rapidly performed with a small hand-held programmable calculator.

Figure 15 shows a summary of the sources expected to contribute to pointing error during off-axis pointing when the gate positions are updated at one minute intervals. The misalignment and gate deadband are similar to those associated with on-axis tracking. The bias or uncertainty in the calculation of the guide star rotation rate will cause an error that will build up during the pointing interval and this is shown as the rate estimate uncertainty error. The time increment error represents the motion of the guide star between gate position updates and is independent of the pointing interval length. The video nonlinearity error arises from the motion of the guide star from the initial position; gondola pendulation will cause a small apparent movement of the guide star and is shown as the gondola disturbance error. Figure 15 shows that the pointing error during a one-hour interval with the guide star two degrees from the object will be less than 1.29 arc minutes.

Examining Figure 15 reveals that if the more complex method of updating the gate positions with an on-line ground station computer were used, the rate estimate uncertainty and time increment errors would be removed. The one sigma pointing error would then be 0.73 arc minutes for the one-hour interval.

CONCLUSIONS

The AIROscope pointing and stabilization system has been configured with rate integrating gyros, direct drive torque motors and three gimbals to provide a very stable platform for infrared astronomy. Since the azimuth torque motor uses the suspension for reaction torque, a tachometer and control logic have been implemented to increase the suspension damping. The use of an electronic integrator, in the elevation and cross elevation RIG stabilization loops, aids in the rejection of disturbance torques and minimizes the effect of pendulation disturbances coupling through bearing stiction and torque motor back emf. A unique video sensor provides error signals for on and off-axis pointing and information for a CRT display in the ground station. Results of the pointing error analysis show that the on-axis pointing error should be less than 0.51 arc minutes, and that the off-axis pointing error should be less than 1.29 arc minutes for pointing intervals up to one hour.

ERROR SOURCE	arcmin	CONFIDENCE	1σ
MISALIGNMENT	0.50	1σ	0.50
GATE DEADBAND	0.35	3σ	0.12
RATE ESTIMATE UNCERTAINTY	3.14	3σ	1.05
TIME INCREMENT 1 STEP/min	0.52	3σ	0.17
VIDEO NONLINEARITY	0.20	1σ	0.20
GONDOLA DISTURBANCE	1.40	3σ	0.47

GUIDE STAR 2° FROM OBJECT

1 σ RSS TOTAL = 1.29 arcmin
FOR 1 hr INTERVAL

Figure 15. Off-Axis Pointing Error

SYMBOL	
d	Suspension cable separation
H	RIG angular momentum
J_1	Suspension inertia
J_2	Azimuth inertia
J_3	RIG gimbal and wheel inertia
J_4	Elevation inertia
K_a	Acceleration constant for evaluation of rate gyro errors
K_B	Coefficient of azimuth bearing friction and torque motor back emf
K_{BE}	Coefficient of elevation torque motor back emf
K'_{B1}	Coefficient of azimuth damping during slewing
K'_{B2}	Coefficient of azimuth damping during stabilization
K_G	RIG position feedback gain
K_I	Elevation torque motor scale factor
K_{MI}	Tachometer scale factor
K_{MZ}	RIG scale factor
K_P	Position scale factor
K_R	Balloon rotation rate constant
K_{TM}	Azimuth torque motor scale factor
K_v	Rate scale factor
K_z	Coefficient of RIG gimbal damping
K_r	Coefficient of suspension torque
L	Suspension cable length
M	Gondola and telescope weight
M_c	Control torque
M_{D1}	Suspension disturbance torque
M_{D2}	Azimuth gimbal disturbance torque
M_s	Stiction torque
R	Elevation torque motor winding resistance
T_d	Elevation gimbal disturbance torque
T_s	Video sensor sample rate
W_g	Gondola pendulation rate

θ_1	Suspension angle
θ_2	Azimuth gimbal angle
θ_3	Elevation gimbal angle
θ_r	$\theta_1-\theta_2$
γ_s	Time constant
SGN	Signum function

REFERENCES

Deboo, G.J., Parra, G.T., and Hedlund, R.C., 1974. The AIROscope Stellar Acquisition System. Symposium on Telescope Systems for Balloon-borne Research. To be published.

Frecker, J.E., 1968. The Polariscope Balloon-borne Servo System. LPL Communications No. 109.

Greeb, M.E., and True, G.A., 1974. Balloon Infrared Astronomy Platform (BIRAP). Symposium on Telescope Systems for Balloon-borne Research. To be published.

Koontz, O.L., and Scott, S.G., 1974. AIROscope Ames Infrared Balloon-borne Telescope. Symposium on Telescope Systems for Balloon-borne Research. To be published.

Morris, A.L., and Stefan, K.H., 1969. High Altitude Balloons as Scientific Platforms. NCAR, Boulder. 85p.

Nidey, R.A., 1969. International Orbital Laboratory and Space Sciences Conference. International Academy of Astronautics, Cloudcraft. 9p.

Nidey, R.A., 1966. Stabilization and Orientation of Balloon-borne Instruments. Kitt Peak National Observatory, Tucson. 36p.

DISCUSSION SUMMARY — PAPER 4.6

Information about the weight, cost and power consumption of the rate integrating gyros was requested. The gyros used on AIROscope are surplus units costing $400 each. They were bought from commercial surplus dealers. They weigh approximately one-half kilogram. Their power consumption is less than 10 watts. Most of this power is for the heaters.

It was noted that the gimbal arrangement does not allow for correction of field rotation.

A question was asked regarding a comparison of calculated performance with the performance of the gyroscope. This, of course, depends on how one corrects for drift in the gyroscopes. If this is done with a star tracker (observing an on-axis object) as in the original Polariscope, 15 arcseconds pointing accuracy could be expected. In the infrared where off-axis tracking is often necessary the TV camera is used for the drift correction, but it is less accurate than on-axis tracking.

The speaker noted that many of the ideas used on AIROscope, such as the three gimbals, the video display and the ground station were basically features of the Polariscope system. Since they were considered to be good features, they have been carried over to the new system. The difference in the tracking systems stems from the fact that so many strong IR sources have faint visible counterparts, so that the star tracker is not always useful.